

Nature and number of distinct phases in the random field Ising model

Jairo Sinova^{1,2,3}, Geoff Canright^{1,2,4}

¹*Department of Physics, University of Tennessee, Knoxville, Tennessee 37996*

²*Department of Physics, Indiana University, Bloomington, Indiana 47405-4201*

³*Department of Physics, The University of Texas, Austin, Texas 78712-1081*

⁴*Physics Institute, University of Oslo, Norway*

(October 26, 2018)

We investigate the phase structure of the random-field Ising model with a bimodal random field distribution. Our aim is to test for the possibility of an equilibrium spin-glass phase, and for replica symmetry breaking (RSB) within such a phase. We study a low-temperature region where the spin-glass phase is thought to occur, but which has received little numerical study to date. We use the exchange Monte-Carlo technique to acquire equilibrium information about the model, in particular the $P(q)$ distribution and the spectrum of eigenvalues of the spin-spin correlation matrix (which tests for the presence of RSB). Our studies span the range in parameter space from the ferromagnetic to the paramagnetic phase. We find however no convincing evidence for any equilibrium glass phase, with or without RSB, between these two phases. Instead we find clear evidence (principally from the $P(q)$ distribution) that there are only two phases at this low temperature, with a discontinuity in the magnetization at the transition like that seen at other temperatures.

I. INTRODUCTION

The random-field Ising model (RFIM) is one of the simplest problems that one can define theoretically in which disorder is present and plays a significant role in the physics. This problem gains further interest since a related random system which may be realized experimentally—namely, the site-diluted antiferromagnet in a uniform field—may be mapped onto the RFIM. The RFIM has been subjected to considerable study, both experimental and theoretical, for over 25 years [1]. Much effort has been focussed on the nature of the phase diagram. It is known rigorously that, for low temperatures and low random fields, the ferromagnetic (FM) phase found in the pure system survives for $d \geq 3$ (where d is the space dimension). However most other questions that one can ask about this system for $d = 3$ (hence beyond the range of validity of mean-field theory) remain unanswered. For example, is the phase transition first-order or continuous? Is there a tricritical point, separating a critical line from a line of first-order transitions? Does the answer to these questions, and/or the universality class of the critical line, depend on the distribution of random fields? And finally: is there a third, spin-glass (SG) phase, in addition to (and likely separating) the FM and paramagnetic (PM) phases?

In this work we focus on this last question. Early numerical studies using mean-field theory [2–4] defined a nonequilibrium “domain state”, characterized by various forms of irreversible behavior, of a similar nature to the irreversible behavior seen experimentally. This irreversibility region, found between the PM and FM phases, gives (at most) hints of the presence of an equi-

librium glassy phase. Stronger arguments for a glassy phase were made by de Almeida and Bruinsma [5], who showed that, although mean-field theory in strictly infinite dimension gives replica symmetry [6], in large dimensions there is a stable glassy phase with replica symmetry breaking (RSB). This result is supported by the work of Mezard and Young [7] and of Mezard and Monasson [8], who showed that there is a SG phase with RSB in the limit of a large number of spin components, and by Guagnelli *et al* [9], who showed the presence of multiple solutions to the mean-field equations in $d = 3$, at a temperature well above the FM ordering temperature. Subsequently, Brezin and de Dominicis [10] developed a renormalization-group approach for a replicated theory, and argued for RSB on the basis of a loss of stability of the fixed point. Finally, we mention exact numerical zero-temperature studies [11] which show the appearance of extensive entropy in the ground state at the point where FM order disappears.

Thus there are good reasons to consider the possibility of a SG phase for the RFIM, located between the FM and PM phases, and likely (see [5]) more easily detected at low T and large random field. It is also of great interest to test for the presence of RSB in this phase. To date, conclusive evidence for RSB is confined to theoretical models in infinite dimension; to confirm RSB in a three-dimensional problem—which can be studied experimentally—would be an important step.

In earlier work [12,13] we have developed a method for detecting RSB in finite-size numerical studies. The method relies on examining the eigenvalues of the spin-spin correlation matrix. We showed that, in the limit of large number of spins N , there are multiple $O(N)$ eigen-

values of this matrix, if [13] and only if [12] there is RSB. This was clearly confirmed by Monte-Carlo (MC) studies of the infinite-ranged Sherrington-Kirkpatrick problem, which is known to have RSB. Unfortunately, this method gave no evidence for RSB in a finite-(4)-dimensional version of the same problem.

We apply the same method to the 3-dimensional RFIM in this work. We note that previous numerical studies [14] of phase transitions of the RFIM are almost entirely confined to two regions: either relatively high temperatures and low random fields, or zero temperature. However, based on the location of the irreversibility regions in phase space, and on the results of Ref. [5], one is most likely to find a glassy phase by looking in the high-field, low- T region; this we do here.

Our results, in short, are as follows. We find some, rather ambiguous, evidence for RSB in the behavior of the spin-spin eigenvalues, over a small range of field, at fixed, low temperature. On either side of this region we see clearly the PM and FM phases. Thus this narrow region is either the sought-for glassy phase, or simply the finite-size effects of the phase transition itself. Examination of the order parameter function $P(q)$ enables us to rather conclusively rule out the former explanation in favor of the latter: a FM/PM phase boundary. Finally, we see at the transition the discontinuity (or near-discontinuity [15,16]) in magnetization that has been seen in many other studies, both at zero [17–19] and at higher [20–22] temperature.

We organize the rest of this paper as follows. In Sec. II we briefly explain the general technique of correlation matrix spectral analysis introduced in our previous work [12]. In Sec. III we present the procedures and results of the numerical analysis of the bi-modal RFIM model in a cross-section of the phase diagram. Finally in Sec. IV we present our conclusions.

II. CORRELATION MATRIX SPECTRAL ANALYSIS

In considering frustrated and disordered systems such as spin glasses, one is forced to broaden the concept of ‘ordering’ in describing the frozen phase. The key point, as recognized long ago by Edwards and Anderson [23], is simply the freezing itself: long-time averages become nonzero. One can detect this freezing through correlation functions: if the freezing is long-ranged (i.e., truly a distinct phase), then so are the correlations. Viewing the correlation function as a matrix, one finds that ordering (freezing) appears in the spectrum of the correlation matrix as an extensive (which we will also call ‘large’) eigenvalue [24]. Thus examination of this spectrum allows one to detect ordering/freezing, while completely avoiding any need to guess the *nature* of the ordering

(i.e., the eigenfunction corresponding to the large eigenvalue).

For Ising systems, a suitable correlation function is

$$C_{ij} \equiv \langle S_i S_j \rangle ;$$

this is a real symmetric positive semi-definite matrix with trace equal to the system volume N . In the frozen phase at least one of the eigenvalues of C_{ij} is extensive, i.e., of $O(N)$. For a simple Ising ferromagnet without quenched disorder, freezing leads to the partitioning of spin configuration space into two disjoint regions (+ and –); each is frozen, and each has the same thermodynamic weight since they are related by a symmetry of the Hamiltonian, namely spin inversion. Since C_{ij} is invariant under this symmetry, the two (symmetry breaking) frozen states give only a single large eigenvalue.

In the case of replica symmetry breaking or RSB, there are multiple frozen states which are not related by any symmetry of the Hamiltonian. We have shown [13] that, when there is RSB, there must be more than one extensive eigenvalue in the spectrum of C_{ij} —assuming of course that the thermal average is taken over the entire configuration space. We have also shown [12] that, in the absence of RSB, there can only be one such extensive eigenvalue. Given these results, one can obtain a definitive answer to the question of whether or not a system exhibits RSB, by determining whether there is or is not more than one large eigenvalue in the spectrum.

This latter question is well defined, but is vulnerable to finite-size uncertainties (as are other criteria such as the overlap distribution $P(q)$). Here such uncertainties arise because the definition of an extensive eigenvalue depends on taking the large- N limit. Thus, in numerical studies of finite systems, one must look for convincing evidence that one has indeed found the asymptotic behavior, at least of the two largest eigenvalues of C , as N increases. In particular, one must determine if the second largest eigenvalue λ_2 grows linearly with N at large N . In the absence of RSB, λ_2 can grow [12,13] with N as $\lambda_2 \sim N^{1-\delta}$ with $\delta > 0$. RSB, in contrast, requires that δ be strictly zero.

Let us now discuss these ideas as applied specifically to the RFIM. In the paramagnetic phase (for nonzero values of the random field) there is freezing of the spins, which (on average) simply follow the random field. Thus the frozen configuration is unique, giving a single large eigenvalue. In the ferromagnetic phase there is a + and a – state. However, due to the random field, the two are no longer strictly related by symmetry; nor—due to a net field of $O(N^{1/2})$ —do they have equal thermodynamic weight. (These two states are termed ‘similar but incongruent’ by Huse and Fisher [25].) Hence we again expect a single extensive eigenvalue in the FM phase.

In this work we will look for signs of a spin-glass phase in a low-temperature region between the PM and FM

phases. If the SG phase has RSB—and we are able to study a range of N beyond the threshold [12] for observing RSB—then we should find multiple large eigenvalues of C . Note that, if λ_2/N decays over the entire range of N studied, and reaches a very small value within that range, then that small value offers a rough upper bound for the thermodynamic weight which may be assigned to any putative RSB state. Hence there may be RSB in such a case; but it would be a ‘weak’ RSB, where only one state has large thermodynamic weight. We also do not rule out the possibility of a SG phase without RSB, i.e., with a single large eigenvalue. In this case one needs other measures (such as qualitative changes in the scaling of λ_2/N , in $P(q)$, or in the spin-glass susceptibility χ_{SG}) to distinguish the SG phase from the other two.

III. NUMERICAL PROCEDURES AND RESULTS

A. The numerical method

The RFIM Hamiltonian is given by

$$\mathcal{H} = -J \sum_{\langle ij \rangle} S_i S_j - \sum_i h_i S_i \quad (1)$$

with $\langle ij \rangle$ indicating the sum over nearest neighbors, J being the strength of the ferromagnetic coupling, and h_i being a quenched random variable. In this work we will take $J = 1$, so that temperatures and fields are measured in units of J . The two common probability distributions for h_i are a Gaussian distribution, with variance Δ , or the bi-modal distribution

$$P(h_i) = \frac{1}{2} [\delta(\Delta - h_i) + \delta(\Delta + h_i)] .$$

As we noted in the Introduction, there is some uncertainty as to which features of the phase diagram are sensitive to the choice between these two distributions. For example, Aharony [26] predicts a tricritical point for the bimodal distribution, but not for the Gaussian. We will work with the bimodal distribution, principally because it enables faster Monte-Carlo simulation. Also, we know of no reason to expect that a SG phase is more or less likely to occur for one or the other distribution.

As is the case in all glassy systems, the system sizes of Monte Carlo simulations are severely restricted by long relaxation or equilibration times. The typically long time that it takes to jump across large energy barriers in configuration space can be greatly reduced by the parallel tempering or exchange Monte Carlo technique [27]. This technique consists of running simultaneously multiple replicas of the system at different temperatures, while allowing the swapping of spin configurations between adjacent temperatures. Such swaps are attempted

every N_s Monte Carlo steps. By choosing the probability of swapping correctly—meaning that the probability of a given spin configuration being accepted from another replica at a different temperature is constrained to be consistent with the Boltzmann distribution at the original temperature—all copies of the system remain in equilibrium under the swapping process. This effectively enables the jumping of free-energy barriers, since different replicas are likely to be in different local minima of the free energy.

Another important aspect of Monte Carlo simulations in quenched-disorder systems is a set of robust equilibration criteria, needed to obtain reliable numerical data. The parallel tempering technique does not allow one to use the equilibrium criteria used in Reference [28], in which two methods of calculating the disconnected spin glass susceptibility approach the equilibrium value from different directions. In the case of spin glasses with Gaussian random bonds, a different technique was used to determine the Monte Carlo time needed for equilibrated results [29]. This criterion cannot be used in the RFIM problem, but another one, which can be derived in a similar fashion, can be used for Gaussian distributed random fields. In the spirit of reference [29], it is straightforward to show that

$$q_{EA} = 1 - \frac{T}{N\Delta^2} \sum_i [h_i \langle S_i \rangle_T]_{av} , \quad (2)$$

where $q_{EA} \equiv (1/N) \sum_i [\langle S_i \rangle_T^2]_{av}$ is the Edwards-Anderson order parameter, and $\langle \dots \rangle_T$ and $[\dots]_{av}$ indicate thermal and disorder average respectively. One can calculate q_{EA} numerically using the overlap of two uncorrelated replicas (a and b) at the same temperature,

$$q_{EA}^{(1)} \equiv \frac{1}{Nt_0} \sum_i \sum_{t=1}^{t_0} S_i^{(a)}(t) S_i^{(b)}(t) \quad (3)$$

or by using expression (2) to obtain what we will call $q_{EA}^{(2)}$. These two quantities approach the thermodynamic equilibrium value q_{EA} from opposite directions as t_0 , the number of Monte Carlo steps used, increases. Hence one can use their convergence to a common value as a criterion for the equilibration time.

We have not found an expression analogous to (2) for the case of a bi-modal distribution of fields. We note however that the time evolution of $q_{EA}^{(1)}(t_0)$ for the bimodal case follows that for the Gaussian distribution (using the same parameters) very closely. Therefore, we can take the equilibrating value of t_0 obtained for the Gaussian distribution, and use it for the bi-modal case as a minimum Monte Carlo time needed to reach equilibrium for each disorder configuration. We retain the bi-modal distribution for the bulk of our MC studies as it allows for a faster algorithm.

In Fig. 1 we show the behavior of the two versions of q_{EA} , calculated with a Gaussian distribution for $T/J =$

2.2, $\Delta/J = 0.4$, and $L = 5$. We also show these two quantities for the bi-modal model. It is clear that $q_{EA}^{(2)}$ is not equivalent to $q_{EA}^{(1)}$ in this case. However, as noted above, both $q_{EA}^{(1)}$ and $q_{EA}^{(2)}$ for the bi-modal model plateau at the same point where $q_{EA}^{(1)}$ and $q_{EA}^{(2)}$ meet for the Gaussian model.

As criteria for equilibrium we then have several requirements. First, the equilibration time must be at least twice the time needed to establish convergence of $q_{EA}^{(1)}$ and $q_{EA}^{(2)}$ for the Gaussian case. Second, we require that two distinct ways of computing $\chi_{SG}^{(1)} \equiv \frac{1}{N} \sum_{ij} \langle S_i S_j \rangle_T^2$, one using two replicas at the same temperature and the other a direct Monte Carlo method, agree within statistical error [13].

Our third criterion has to do with the exchange Monte Carlo method. In order to ensure that equilibrium holds for all the various temperatures simulated in parallel, we require that the probability histogram for visiting the different temperatures is flat, and also that the acceptance ratio for swapping among the configurations at different temperatures is at least 0.3. In order to avoid the bottlenecks mentioned in reference [29] with regard to the acceptance ratios among the different temperatures, we follow a procedure introduced by Hukushima [30]. Here we perform a quick Monte Carlo simulation (only a few disorder realizations) with an equidistant set of β 's to obtain an approximation for the average energy of the system. In order to obtain homogeneous acceptance ratios one performs the following mapping:

$$\beta_n(t+1) = \frac{1}{2}[\beta_n(t) + g(\beta_n(t))] , \quad (4)$$

where

$$g(\beta_n) = \frac{1}{E(\beta_{n-1}) - E(\beta_{n+1})} \times [\beta_{n-1}E(\beta_{n-1}) - \beta_{n+1}E(\beta_{n+1}) - E(\beta_n)(\beta_{n-1} - \beta_{n+1})] . \quad (5)$$

Here the values of $E(\beta_i)$ are obtained by extrapolation from the ones obtained in the initial Monte Carlo runs. Using this procedure we obtain a set of temperatures (β 's) that yield homogeneous acceptance probabilities when a swap between two adjacent temperatures is attempted. We can then, if necessary, increase the number of β 's and repeat the procedure, until the uniform swapping probability reaches our minimum goal of at least 0.3. In Fig. 2 we show the swapping acceptance ratios after zero, one, and two iterations of this procedure, for $L = 11$, $T_{min}/J = 1.5$, and $\Delta/J = 0.6$. It is clear from the figure that the bottleneck at $T/J = 4$ is removed by the iterative procedure.

Our final criterion is to require that the maximum temperature used in the parallel tempering process shows a ‘melted’ $P(q)$; that is, $P(q)$ at the smallest β must have an approximate Gaussian shape centered at or near

$q = 0$. This criterion is necessary to ensure that all free-energy barriers have vanished at this β , so that the different thermodynamic states in the low-temperature phase(s) will be visited with a probability corresponding to their thermodynamic weight.

B. Numerical results

As mentioned in Sec. I, there are indications from mean field studies [5,8,7,9] that a SG phase with RSB may exist in an intermediate region of the phase diagram, which roughly coincides with the irreversibility region found in dynamical calculations [2–4]. One can see a hint of this by doing a Monte Carlo simulation, and computing the spectrum of C_{ij} , for a single disorder realization at a relatively small system size (in order for the calculation to be feasible) over the whole phase diagram. We plot the first two eigenvalues of C_{ij} for a single disorder realization in Fig. 3. In the FM and PM phases there is clearly a single large eigenvalue λ_1 , while in a region between the two phases the first two eigenvalues are of the same order of magnitude. This could be due to an intermediate phase with RSB. On the other hand, such behavior could also be due to the FM and PM eigenvectors (which represent two distinct forms of ordering) trading places in the spectrum as one moves from one phase to the other.

We can follow up these hints by studying larger systems, at a single (low) temperature, over a range of fields Δ which spans the intermediate region seen in Fig. 3. Hence we have performed a rather thorough Monte-Carlo scan of the field parameter Δ at a fixed, low temperature $T = 1.5$. For a preliminary coarse scan we studied the values $\Delta/J = 2.0, 3.0$, and 4.0 . The system sizes for each Δ are $L = 5, 7, 9$, and 11 , with the number of disorder realizations being 2000, 2000, 850, and 650, respectively. Previous work [3] has yielded the dynamical phase diagram shown in the inserts of Figs. 4 and 5. Our coarse scan has been chosen to both bracket and sample the irreversibility region, as shown in the inserts in Figs. 4 and 5. In these figures we plot (respectively) the average and typical values (where $[\lambda_i]_{typ} \equiv \exp([\ln \lambda_i]_{ave})$) for the λ_i/N , plotted against N on a log scale. There is a clear power-law falloff of λ_2/N for $\Delta = 3.0$ and 4.0 . The same is not quite true for $\Delta = 2.0$. That is, for $\Delta = 2.0$ the falloff at small N grows weaker ($[\lambda]_{typ}$) or even ceases ($[\lambda]_{av}$) at larger N . Therefore we performed a second, finer scan over the values $\Delta = 1.8, 2.2, 2.3, 2.4$, and 2.6 , with the same number of disorder realizations as given previously.

Results from this scan ($[\lambda_i]_{ave}$ only) are plotted in Fig. 6. The hints of possible RSB seen in Fig. 3 are considerably stronger here, particularly at $\Delta = 2.4$. $\Delta = 1.8$ is clearly in the FM phase. Also, it seems very likely that the falloff of λ_2/N at $\Delta = 2.6$ will persist at larger N .

Hence, we may take $\Delta = 2.6$ to lie in the PM phase. The question is then, have any of the other plots of λ_2/N in Fig. 6 reached asymptotic behavior?

It is in fact impossible to answer this question from examination of Fig. 6 alone. One main problem is the rise in λ_2/N that occurs in many of the plots at small N . This obvious finite-size effect is likely due to the fact that we are not far from one (or two) phase boundaries. Such a rise must be followed by an asymptotic behavior which is either flat or falling; and, as is clear from the $\Delta = 2.6$ plot, the latter can occur. For these reasons the flat region at $\Delta = 2.4$ gives no unambiguous conclusion: it may be just a local maximum in N , or it may be the large- N behavior. And we are equally unsure of the large- N behavior for $\Delta = 2.0$ – 2.3 . Taken as a whole, the six plots in Fig. 6 can be viewed either as an RSB phase developing between two other phases, or as the finite-size effects of a phase transition between two competing order parameters.

We find that this ambiguity is considerably diminished by a study of the equilibrium $P(q)$ distributions for the various Δ values. Figure 7 shows the full $P(q)$ distribution for the same Δ values seen in Fig. 6. The overall impression is clear: two different kinds of order, represented by peaks at different values of the overlap q , are competing (via fluctuations) in the intermediate values of Δ . At the lower end of the scan, $\Delta = 1.8$, the FM phase gives a peak at q very close to one. There is a much smaller peak at q near -1 (not shown in the Figure) which comes from fluctuations into the “wrong” spin ordering, i.e., that which is not favored by the net random field [which is, again, of $O(N^{1/2})$].

At the other extreme ($\Delta = 2.6$) it is equally clear that FM fluctuations (present at small N) disappear at larger N , leaving a clear peak in $P(q)$ at the (lower) q value appropriate to the PM phase. The dying off of these ferromagnetic fluctuations is well correlated with the decay of λ_2/N in Fig. 6.

This interpretation is readily extended to the remaining Δ values. For instance, at $\Delta = 2.2$ in Fig. 7 there are clearly PM fluctuations giving a very broad peak at $q \sim 0.9$. This is even more clear if we expand the negative- q portion of the $P(q)$ plot for the same Δ (Figure 8). Here we see a small peak near $q = -1$ showing overlap between “wrong” and “right” FM states, and an even smaller peak which we ascribe to overlap between “wrong” FM fluctuations and PM fluctuations. Very similar behavior is seen in $P(q)$ for $\Delta = 2.3$ —both at positive and negative q . The main difference is that the PM fluctuations are stronger than they are at $\Delta = 2.2$. Hence we conclude that both of these Δ values lie in the FM phase for the RFIM, and that the growth of λ_2/N with increasing N for these Δ values is purely due to finite size, plus nearness to a phase boundary.

Finally, we see no justification for postulating a distinct thermodynamic phase based on the behavior at the

remaining Δ value ($\Delta = 2.4$). The behavior both of its eigenvalue spectrum, and of its $P(q)$ distribution, is clearly intermediate to the behaviors at lower and higher Δ . Furthermore, its $P(q)$ distribution, viewed on its own, gives no convincing sign of converging towards a distribution appropriate for a spin glass. In fact, the trend with N (Fig. 7) shows that the PM peak is steadily growing with N , at the expense of the FM peak. This is, again, a picture of competition between two forms of order (each rather strong) near a phase transition, rather than a distinct phase. Furthermore, if one plots the total weight at negative q [that is, the integral $I_- = \int_{-1}^0 dq P(q)$] against N for the various Δ values, one finds very similar behavior for $\Delta = 2.6$ and 2.4 : I_- falls very fast, reflecting the fact that the “wrong” FM fluctuations vanish rapidly with increasing system size. For all of these reasons, we tentatively assign $\Delta = 2.4$ to the PM phase.

Figs. 6, 7, and 8, viewed together, give, we believe, a rather clear picture. There are two phases—FM and PM—of the bimodal RFIM at $T = 1.5J$. The transition between these two phases occurs (probably) between $\Delta = 2.3$ and 2.4 .

There is a further conclusion which seems obvious from the above considerations, and from Fig. 7. The location (in q) of the peak in q , for the FM phase, shows no sign of going to zero as the transition is approached from below. Hence, either the magnetization is discontinuous at the phase boundary [17–22] or it is continuous, but with an extraordinarily small exponent β [15,16], such that it is ‘practically’ discontinuous. Obviously, our numerical studies cannot distinguish these two possibilities. However, this aspect of the behavior of $P(q)$ at $T = 1.5$ —that is, the abrupt vanishing of the magnetization at the transition—is completely consistent with the behavior seen at higher temperatures (closer to the pure critical point) and at zero temperature. This consistency, we believe, adds further support to our claim that there is no new, third phase in the part of the phase diagram studied here.

IV. CONCLUSION

The above results and reasoning have presented a rather clear picture: there is no spin-glass phase, and no replica symmetry breaking, for the bimodal random-field Ising model in the low-temperature region that we have examined. One of the tests that we have applied was to study the scaling with N of the spectrum of eigenvalues of the spin-spin correlation function C_{ij} . We have used this technique previously [12,13] to give unambiguous confirmation of RSB in a case (the Sherrington-Kirkpatrick problem in infinite dimension) where it is strongly believed to occur, and also to give strong evidence against RSB for a finite-dimensional version of the same problem (for which there is still controversy). Here we have sought

evidence for RSB in a different problem, the RFIM—which may be mapped to the diluted antiferromagnet in an external field, a system which may be studied experimentally. We have found that the eigenvalue spectrum gives no sign at all of RSB over most of the range of random field strength Δ that we have studied. There is a small range of Δ for which the behavior of this spectrum is ambiguous. However examination of the overlap distribution $P(q)$ removes the ambiguity, giving instead clear evidence for a single phase transition between the FM and PM phases, with no intervening equilibrium phase. Hence we view the behavior of the eigenvalue spectrum (Figs. 3 and 6) in this intermediate region as purely the finite-size effects of closeness to a phase boundary. In particular, the failure of λ_2/N to decay for this range of fields Δ , even out to $N = 1331$ spins, stems from the persistence of fluctuations between two adjacent phases, each with a large order parameter. Hence we speculate that the eigenvalues would behave less ambiguously—i.e., they would display a reduced tendency to mimic RSB—if the transition were continuous in a conventional sense, such that the order parameters on either side vanished more smoothly.

It is possible (although, we feel, very unlikely) that studies at larger system sizes may reveal these conclusions to be wrong, confirming instead a spin-glass phase confined to a narrow range of Δ at low T . A more promising direction for future work might be to examine the RFIM with a Gaussian distribution of fields, since it remains possible that the two problems have differing phase diagrams. Also, one might argue that a SG phase is suppressed by the strength of the order parameters on each side of the transition. By this argument, one should look at higher T , closer to the pure critical point. However, both nonequilibrium [2–4] and equilibrium [5] mean-field arguments point to the low-temperature region as being most likely to support a spin glass phase. This is why we looked at low T ; and our results rather clearly imply only two phases there.

The authors acknowledge helpful discussions with A. Aharony, H. Castillo, and E. Fradkin. GSC thanks the Theory Group, Physics Institute, University of Oslo, for hospitality. This work was supported by the National Science Foundation under Grant DMR-9820816 and the Welch Foundation.

-
- [1] For a recent review see T. Nattermann, in *Spin Glasses and Random Fields*, A.P. Young, editor (World Scientific, Singapore, 1997).
 - [2] H. Yoshizawa and D. P. Belanger, Phys. Rev. B **30**, 5220 (1984).
 - [3] C. Ro, G. S. Grest, C. M. Soukoulis, and K. Levin, Phys.

- Rev. B **31**, 1682 (1985).
- [4] G. S. Grest, C. M. Soukoulis, and K. Levin, Phys. Rev. B **33**, 7659 (1986); U. Nowak and K. D. Usadel, Phys. Rev. B **44**, 7426 (1991).
- [5] J. R. L. de Almeida and R. Bruinsma, Phys. Rev. B **35**, 7267 (1987).
- [6] T. Schneider and E. Pytte, Phys. Rev. B **15**, 1519 (1977).
- [7] M. Mezard and A. P. Young, Europhys. Lett. **18**, 653 (1992).
- [8] M. Mezard and R. Monasson, Phys. Rev. B **50**, 7199 (1994).
- [9] M. Guagnelli, E. Marinari, and G. Parisi, J. Phys. A **26**, 5675 (1993); D. Luncaster, E. Marinari, and G. Parisi, J. Phys. A **28**, 4481 (1995).
- [10] E. Brézin and C. De Dominicis, Europhys. Lett. **44**, 13 (1998); and cond-mat/0007457.
- [11] S. Bastea and P.M. Duxbury, Phys. Rev. E **58**, 4261 (1998).
- [12] Jairo Sinova, Geoff Canright, and A. H. MacDonald, Phys. Rev. Lett. **85**, 2609 (2000).
- [13] Jairo Sinova, Geoff Canright, Horacio E. Castillo, and A. H. MacDonald, Phys. Rev. B **63**, 104427 (2001).
- [14] See, for example, Fig. 3 of M. Itakura, cond-mat/0012488, which shows the range in the phase diagram of several previous numerical studies.
- [15] A. Falicov, A.N. Berker, and S.R. McKay, Phys. Rev. B **51**, 8266 (1995).
- [16] A.T. Ogielski, Phys. Rev. Lett. **57**, 1251 (1986).
- [17] A.K. Hartmann and U. Nowak, Eur. Phys. J. B **7**, 105 (1999).
- [18] J.-C. Anglès d'Auriac and N. Sourlas, Europhys. Lett. **39**, 473 (1997).
- [19] M.R. Swift, A.J. Bray, A. Maritan, M. Cieplak, and J.R. Banavar, Europhys. Lett. **38**, 273 (1997).
- [20] J. Machta, M.E.J. Newman, and L.B. Chayes, Phys. Rev. E **62**, 8782 (2000).
- [21] H. Rieger, Phys. Rev. B **52**, 6659 (1995); H. Rieger and A.P. Young, J. Phys. A **26**, 5279 (1993).
- [22] A.P. Young and M. Nauenberg, Phys. Rev. Lett. **54**, 2429 (1985).
- [23] S. F. Edwards and P. W. Anderson, J. Phys. F **5**, 965 (1975).
- [24] Analogous behavior occurs in superfluids. Here the quantity which ‘freezes’ is a creation or annihilation operator, and the analog of our C_{ij} is a one- (bosons) or two- (superconductors) particle density matrix. The signature of the freezing is again an extensive eigenvalue of the density matrix. See C. N. Yang, Rev. Mod. Phys. **34**, 694 (1962).
- [25] D.A. Huse and D.S. Fisher, J. Phys. A **20**, L997 (1987).
- [26] A. Aharony, Phys. Rev. B **18**, 3318 (1978).
- [27] K. Hukushima and K. Nemoto, J. Phys. Soc. Japan **65**, 1604 (1996); K. Hukushima, Phys. Rev. E **60**, R1008 (2000).
- [28] R. N. Bhatt and A. P. Young, Phys. Rev. B **37**, 5606 (1985).
- [29] Helmut G. Katzgraber, Matteo Palassini and A. P. Young, cond-mat/0007113.
- [30] K. Hukushima, Phys. Rev. E **60**, 3606 (1999).

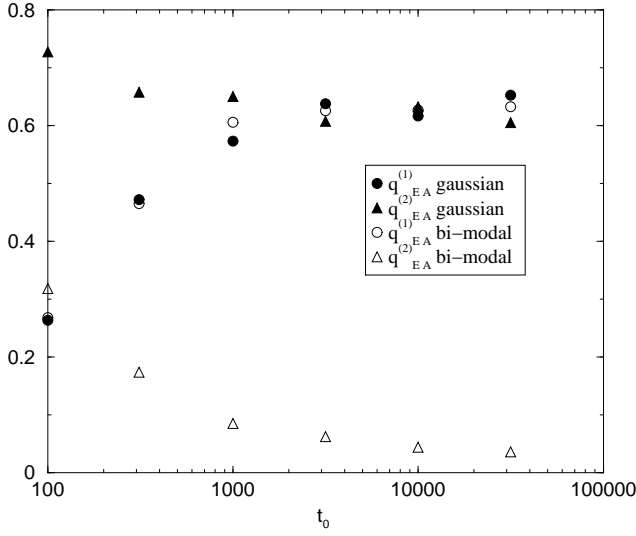


FIG. 1. $q_{EA}^{(1)}$ and $q_{EA}^{(2)}$ vs. Monte Carlo time t_0 for $T/J = 2.2$, $\Delta/J = 0.4$, and $L = 5$. Here we show each quantity for the bi-modal (open symbols) and Gaussian (filled symbols) random field distribution.

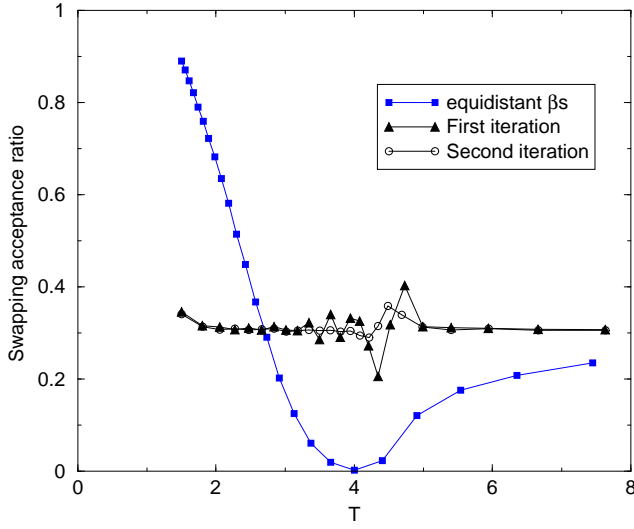


FIG. 2. Swapping acceptance ratios among the configurations at different temperatures at different stages in the iteration defined by Eqs. (4) and (5). Here $L = 11$, $T_{min}/J = 1.5$, and $\Delta/J = 0.6$.

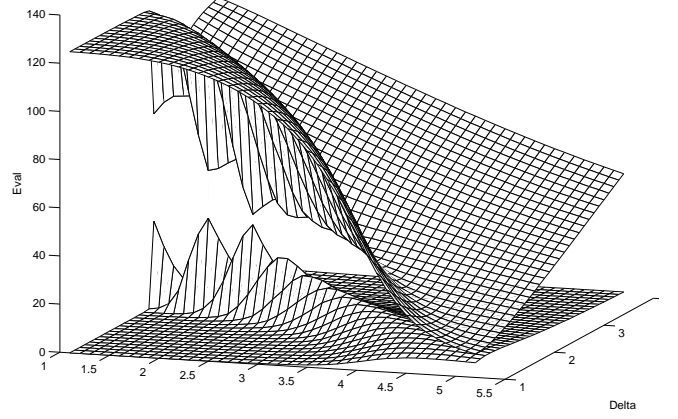


FIG. 3. The first (upper sheet) and second (lower sheet) eigenvalue of the spin-spin correlation matrix for a single disorder realization. The x-axis is temperature (label not indicated). Here $N = 125$. The FM phase lies in the front left corner (small T and Δ), where $\lambda_2 \ll \lambda_1$. The PM phase lies on the other side of the “ridge” in λ_2 ; in the PM phase it is again true that $\lambda_2 \ll \lambda_1$. The ridge in λ_2 , with the corresponding “trough” in λ_1 , may indicate a distinct thermodynamic phase; or it may simply indicate the effects of the FM/PM phase transition.

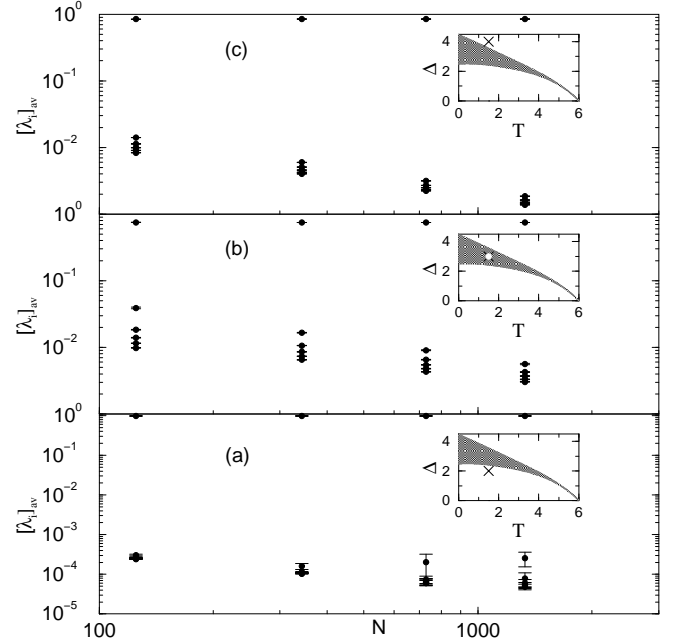


FIG. 4. Scaling of the average of the first six eigenvalues λ_i as a function of N at $T/J = 1.5$ and $\Delta/J = 2.0$ (a), 3.0 (b), and 4.0 (c). The location in the phase diagram obtained through dynamical Monte Carlo obtained from reference 3 is shown in the insert (here $J = 1$).

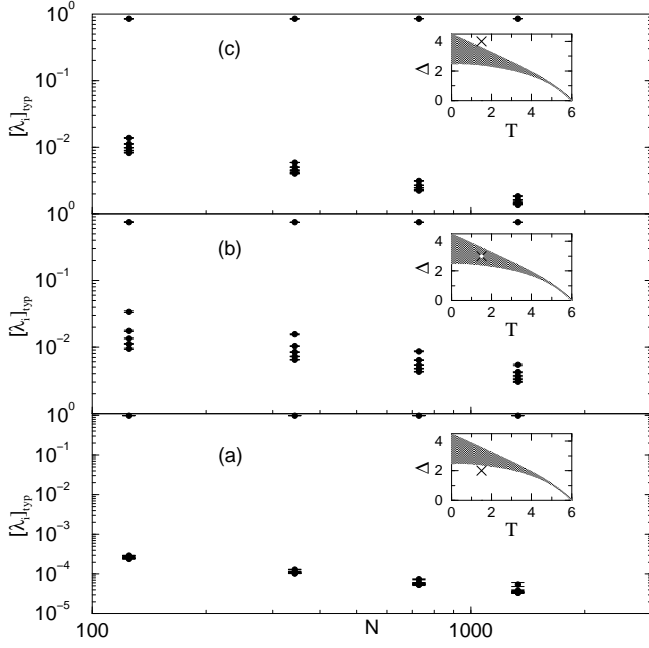


FIG. 5. Scaling of the typical ($[\lambda_i]_{\text{typ}} \equiv \exp(\ln \lambda_i)_{\text{ave}}$) of the first six eigenvalues as a function of N at $T/J = 1.5$ and $\Delta/J = 2.0$ (a), 3.0 (b), and 4.0 (c). The location in the phase diagram obtained through dynamical Monte Carlo obtained from reference 3 is shown in the insert (here $J = 1$). Note that, in this figure and in Figure 4, the falloff of λ_2 with N becomes *weaker* at larger N for $\Delta = 2.0$.

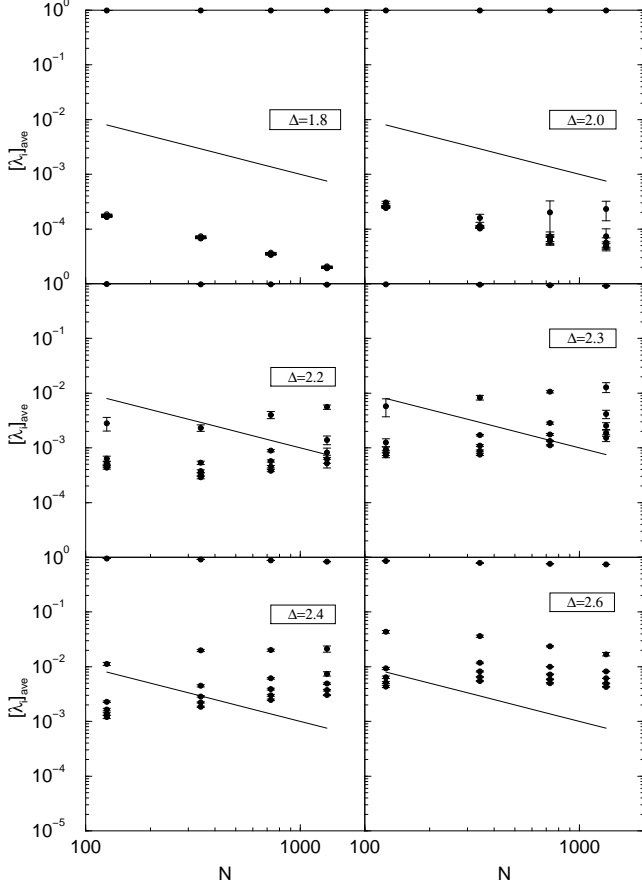


FIG. 6. Scaling of the first six eigenvalues (disorder averaged) at $T = 1.5$, with Δ values as shown. The straight line, $y = 1/N$, is included as a reference for the eye.

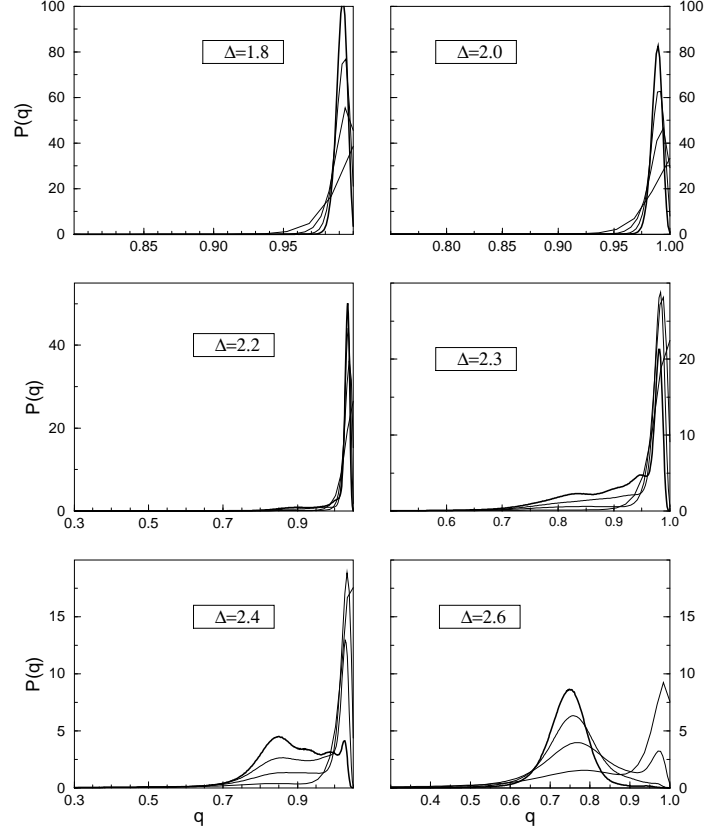


FIG. 7. The overlap probability distribution $P(q)$, plotted for various Δ (as indicated) and system size. The heavy curves correspond to the largest size, $L = 11$. Curves (light lines) for $L = 5, 7$, and 9 may be located by noting that, almost everywhere in q , the curves monotonically approach the $L = 11$ curve. Note that, for clarity, almost every plot uses a different range on each axis.

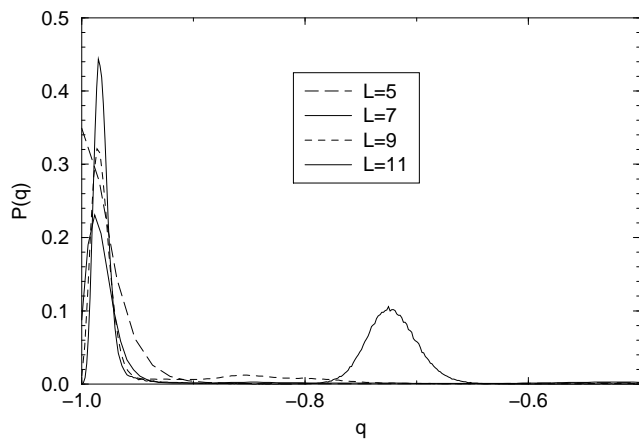


FIG. 8. $P(q)$ for $\Delta = 2.2$, $-1 \leq q \leq -0.5$. At the largest L ($L = 11$) we see two small (compare the vertical scale with Fig. 7) but distinct peaks, which we ascribe to the overlap of “wrong-sign” FM fluctuations with “right-sign” FM ordering (leftmost peak), and of “wrong” FM fluctuations with fluctuations into the paramagnetic phase (peak at $q \sim -0.73$).